CCFM prediction on forward jets and F_2: parton level predictions and a new hadron level Monte Carlo generator CASCADE

H. Jung
Physics Department, Lund University, Box 118, S-221 00 Lund, Sweden

Abstract: A solution of the CCFM equation for a description of both the structure function F_2 and the cross section of forward jet production as measured by the HERA experiments is obtained on the basis of the parton level Monte Carlo program SMALLX. The treatment of the non - Sudakov form factor and the so - called "consistency constraint" are discussed. Following this a backward evolution scheme according to CCFM is developed which then is used to construct an efficient hadron level Monte Carlo program CASCADE. The results from the forward evolution and the backward evolution Monte Carlos are compared and found to be consistent.

1 Introduction

The parton evolution at small values of x is believed to be best described by the CCFM evolution equation [1–4], which for $x \to 0$ is equivalent to the BFKL evolution equation [5–7] and for large x reproduce the standard DGLAP equations. The CCFM evolution equation takes coherence effects of the radiated gluons into account via angular ordering.

Already in 1992 the CCFM evolution equation was implemented in the parton level Monte Carlo program, SMALLX [8,9], using a forward evolution scheme. In 1997 the Linked Dipole Chain [10–13] and the corresponding LDC hadron level Monte Carlo program were developed based on a reformulation of the original CCFM equation. Predictions of the CCFM equation for hadronic final state properties were studied in [14], paying special attention to non-leading effects. Common to all three approaches was the difficulty to describe the structure function F_2 and the cross section of forward jet production in deep inelastic scattering at the same time [10–15].

This article is divided into two parts: In the first part I shall describe briefly the implementation of the CCFM evolution equation into the program SMALLX [8,9], and discuss the treatment of the non-Sudakov form factor Δ_{ns} as well as the effects of the so-called "consistency constraint", which was found to be necessary to include non-leading contributions to the BFKL equation [16]. Then I demonstrate that a proper treatment of the non-Sudakov form factor is essential to achieve a good description of F_2 and the forward jet data at the same time.
In the second part I describe a model for a backward evolution scheme according to the CCFM equation, which forms the basis of the new hadron level Monte Carlo generator CASCADE. One ingredient in this approach is the determination of the unintegrated gluon density function, which is obtained from the forward evolution in SMALLX. As a check of consistency I compare results obtained from SMALLX with those from CASCADE and show nice agreement.

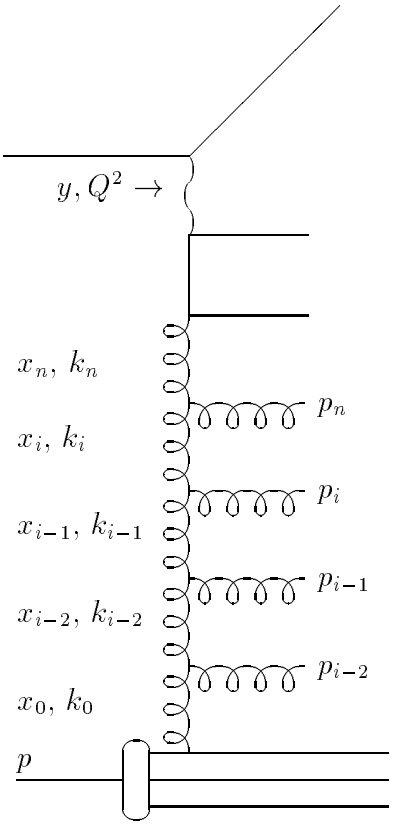

Figure 1: Kinematic variables for multi-gluon emission. The t-channel gluon four - vectors are given by k_i and the gluons emitted in the initial state cascade have four - vectors p_i.

2 Forward evolution: CCFM and SMALLX

The implementation of the CCFM [1–4] parton evolution in the forward evolution Monte Carlo program SMALLX is described in detail in [8,9]. Here I only concentrate on the basic ideas and discuss the treatment of the non-Sudakov form factor.

The initial state gluon radiation is sketched in Fig. 1 together with a definition of some variables used in the following. According to the CCFM evolution equation, the emission of partons during the initial cascade is only allowed in an angular ordered phase space region. The maximum allowed angle Ξ is defined by the hard scattering quark box, which connects the gluon to the virtual photon. In terms of Sudakov variables the quark pair momentum is written as:

$$p_q + p_{\bar{q}} = Y(p_p + \Xi p_e) + Q_t \tag{1}$$

where p_p and p_e are the proton and electron momenta, respectively and Q_t is the transverse momentum of the quark pair. Similarly, the momenta p_i of the gluons emitted during the initial state cascade are given by (here treated massless):

$$p_i = y_i(p_p + \xi_i p_e) + p_{ti} \ , \ \ \xi_i = \frac{p_{ti}^2}{s y_i^2}, \tag{2}$$

with $y_i = (1 - z_i)x_{i-1}$ and $x_i = z_i x_{i-1}$ and $s = (p_p + p_e)^2$ being the total electron proton center of mass energy. The variable ξ_i is connected to the angle of the emitted gluon with respect to the incoming proton and x_i and y_i are the momentum fractions of the exchanged and emitted gluons, while z_i is the momentum fraction in the branching $(i-1) \rightarrow i$ and p_{ti} is the transverse momentum of the emitted gluon.

The angular ordered region is then specified by:

$$\xi_0 < \xi_1 < \cdots < \xi_n < \Xi \tag{3}$$

which becomes:

$$z_{i-1} q_{ti-1} < q_{ti} \tag{4}$$

when using the rescaled transverse momenta q_{ti} of the emitted gluons defined by:

$$q_{ti} = x_{i-1}\sqrt{s\xi_i} = \frac{p_{ti}}{1-z_i} \tag{5}$$

In SMALLX, the initial state gluon cascade is generated in a forward evolution approach from a initial distribution of the k_t unintegrated gluon distribution according to:

$$xG_0(x, k_{t\,0}^2) = N \cdot (1-x)^4 \cdot \exp\left(-k_{t\,0}^2/k_0^2\right) \tag{6}$$

where N is a normalization constant. The exponential factor in eq.(6) is a gaussian distribution which specifies the distribution of the initial transverse momenta $k_{t\,0}$. In the following we set $k_0^2 = 1$ GeV^2, corresponding to a gaussian width of $\sigma = k_0/\sqrt{2} = 0.7$ GeV. The input gluon distribution needs to be adjusted to fit existing data, but it turns out that the small x behavior of the structure function F_2 is rather insensitive to the actual choice of $xG_0(x, k_t^2)$ and only the normalization N acts as a free parameter.

The initial state branching of a gluon k_i into another virtual (t-channel) gluon k_{i+1} and a final gluon p_{i+1} (treated on mass shell) is generated successively from the inital gluon distribution at a starting scale Q_0. The probability for successive branchings to occur is given by the CCFM splitting function [1–4]:

$$dP_i = \tilde{P}_g^i(z_i, q_i^2, k_{ti}^2) \cdot \Delta_s dz_i \frac{d^2 q_i}{\pi q_i^2} \cdot \Theta(q_i - z_i q_{i-1}) \cdot \Theta(1 - z_i - \epsilon_i) \tag{7}$$

with $q_i = p_{ti}/(1-z_i)$ being the rescaled transverse momentum of the emitted gluon i. The fractional energy of the exchanged gluon i is given by x_i and the energy transfer between the exchanged gluon $i-1$ and i is given by $z_i = x_i/x_{i-1}$. A collinear cutoff $\epsilon_i = Q_0/q_i$ is introduced to avoid the $1/(1-z)$ singularity. The Sudakov form factor Δ_s is given by:

$$\Delta_s(q_i, z_i q_{i-1}) = \exp\left(-\int_{(z_{i-1}q_{i-1})^2}^{q_i^2} \frac{dq^2}{q^2} \int_0^{1-Q_0/q} dz \frac{\bar{\alpha}_s(q^2(1-z)^2)}{1-z}\right) \tag{8}$$

with $\bar{\alpha}_s = \frac{C_A \alpha_s}{\pi} = \frac{3\alpha_s}{\pi}$. The Sudakov form factor cancels at an inclusive level against the $1/(1-z)$ collinear singularity of the splitting function. Coherence effects are taken into account by angular ordering $q_i > z_{i-1}q_{i-1}$ given by the first Θ function in eq.(7). The distribution of successive values of q_i is controlled by this Sudakov form factor. The cascade continues until q_i reaches P_{max}, which is given by the partons from the hard scattering matrix element.

The gluon splitting function $\tilde{P}_g^i$ is given by:

$$\tilde{P}_g^i = \frac{\bar{\alpha}_s(q_i^2(1-z_i)^2)}{1-z_i} + \frac{\bar{\alpha}_s(k_{ti}^2)}{z_i}\Delta_{ns}(z_i, q_i^2, k_{ti}^2) \tag{9}$$

with k_{ti} being the transverse momentum of the exchanged gluon i and the non-Sudakov form factor Δ_{ns} being defined as:

$$\log \Delta_{ns} = -\bar{\alpha}_s(k_{ti}^2) \int \frac{dz'}{z'} \int \frac{dq^2}{q^2} \Theta(k_{ti} - q)\Theta(q - z'q_{ti}) \tag{10}$$

The difference to the DGLAP splitting function for gluons is the appearance of the non-Sudakov form factor Δ_{ns}, which screens the $1/z$ singularity in eq.(9). The finite terms in the splitting function are neglected, since they are not obtained in CCFM at the leading infrared accuracy [3, p.72]. In the region $k_{ti}^2 > z_i q_i^2$, Δ_{ns} can be written as:

$$\log \Delta_{ns} = -\bar{\alpha}_s(k_{ti}^2) \log\left(\frac{1}{z_i}\right) \log\left(\frac{k_{ti}^2}{z_i q_i^2}\right) \tag{11}$$

where the limits of the z' integral in eq.(10) were set to $z_i < z' < 1$. However, the Θ functions in eq.(10) give further constraints on the upper limit of the z' integral[1]:

$$z_i \leq z' < z_0 = \max\left(1, \frac{k_{ti}}{q_{ti}}\right) \tag{12}$$

In the region $z_i > k_{ti}/q_i$, the z' integral becomes zero. Putting all this together the non-Sudakov form factor can be expressed as [17]:

$$\log \Delta_{ns} = -\frac{\alpha_s(k_{ti}^2)}{2\pi} \log\left(\frac{z_0}{z_i}\right) \log\left(\frac{k_{ti}^2}{z_0 z_i q_i^2}\right) \tag{13}$$

where

$$z_0 = \begin{cases} 1 & \text{if } k_{ti}/q_i > 1 \\ k_{ti}/q_i & \text{if } z_i < k_{ti}/q_i \leq 1 \\ z_i & \text{if } k_{ti}/q_i \leq z_i \end{cases}$$

which means that in the region $k_{ti}/q_i \leq z_i$ we have $\Delta_{ns} = 1$, giving no suppression at all.

The use of eq.(11) in the region $k_{ti}^2 \leq z_i q_i^2 = z_i p_{t\,i}^2/(1 - z_i)^2$ would result in a change of the sign, and therefore instead of giving a suppression form factor would give an enhancement, which is in contradiction to a form factor. The constraint[2] $k_{ti}^2 > z_i q_i^2$ is often referred to as the "consistency constraint" [16].

In the original version of SMALLX [8,9] the splitting function was defined as:

$$\tilde{P}_g^i = \frac{\bar{\alpha}_s(q_i^2(1 - z_i)^2)}{1 - z_i} + \frac{\bar{\alpha}_s(k_{ti}^2)}{z_i} \frac{\Delta_{ns}(z_i, q_i^2, k_{ti}^2)}{\int dz' \Delta_{ns}(z', q_i^2, k_{ti}^2)} \tag{14}$$

which also is valid over the full phase space, but gives only very weak suppression of the small z splittings, and therefore overshoots the measured structure function F_2 at small values of x.

The Monte Carlo program SMALLX [8,9] has been modified to include the non-Sudakov form factor according to eq.(13) and k_t^2 was used as the scale in α_s also in the matrix element. To

[1] I am very grateful to J. Kwiecinski for the explanation of these limits

[2] The constraint: $Q_{i-1}^2 < Q_i^2/z_i$ was already derived in [18, eq.(2.11)] and in [19] in a frame where parton i is along the z axis. In [3] this was used to derive a similar condition on the transverse momenta (see [3, eq.(7.23)]) $k_t^2 > zq^2$, when the transverse momenta are the dominant contribution to the virtualities. However, in a different frame (the lab frame used in CCFM for example), the numerical value of z might be different, this constraint might be violated.

avoid problems at small k_t^2, a upper limit on α_s was introduced such that $\alpha_s(k_{ti}^2) \leq 0.6$. This modified version of SMALLX is called SMMOD in the following.

A few words are needed concerning the "consistency constraint", which was introduced to account for next-to-leading effects in the BFKL equation. Including this constraint it was found in [16], that about 70% of the full next-to-leading order corrections to the BFKL equation are simulated. However, in LO BFKL the true kinematics of the branchings are neglected. They are included only in NLO therefore act as next-to-leading order effects. Therefore this constraint is often also called "kinematic constraint". In the CCFM equation energy and momentum conservation is already included at LO by the full treatment of the radiated gluons, and it is not clear, whether the arguments coming from BFKL also apply to CCFM.

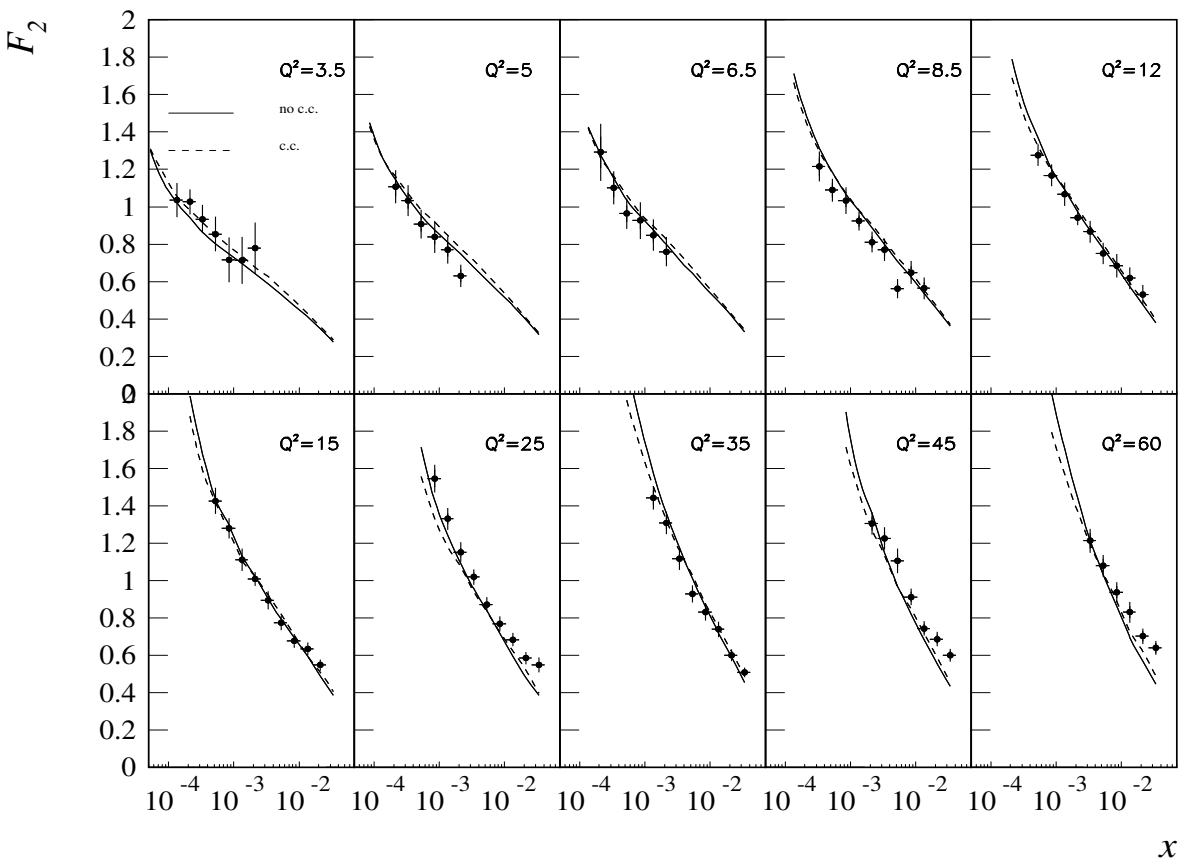

Figure 2: *The structure function $F_2(x, Q^2)$ compared to H1 data [20]. The solid (dashed) line is the prediction of the* SMMOD *Monte Carlo without (with) applying the "consistency constraint" (c.c.).*

In the following the effects of the "consistency constraint" are studied in more detail. In Fig. 2 the structure function $F_2(x, Q^2)$ as calculated from SMMOD (including the non-Sudakov form factor according to eq.(13)) is shown. The solid curve is without the "consistency constraint", the dashed curve shows the result after applying the "consistency constraint". The collinear cutoff Q_0 was set to $Q_0 = 1.1(0.85)$ GeV (without (with) "consistency constraint", respectively). The values of Q_0 have been chosen such, that a reasonable description of F_2 is obtained. In Fig. 3 the cross section of forward jet production and the measurements of [21–23]

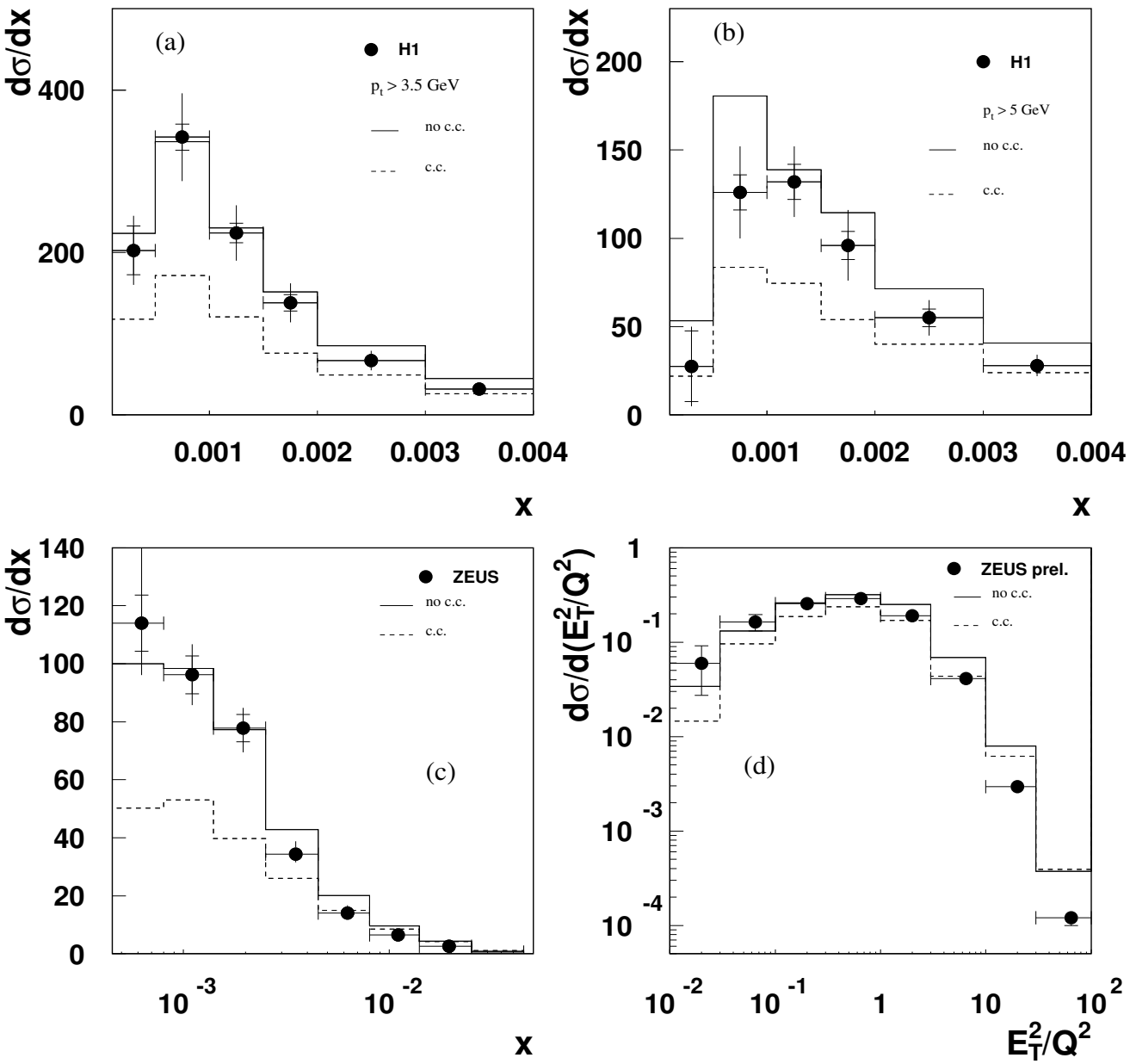

Figure 3: *a.* $-$ *c. The cross section for forward jet production as a function of* x*, for different cuts in* p_t *compared to H1 data [21] (a.*$-$*b.) and compared to ZEUS data [22] (c.). d. The cross section for forward jet production as a function of* E_T^2/Q^2 *compared to [23]. The solid (dashed) line is the prediction of the* SMMOD *Monte Carlo without (with) applying the "consistency constraint" (c.c.).*

are shown as a function of x (Fig. 3a.-c.) and as a function of E_T^2/Q^2 (Fig. 3d.), using the same parameter setting as for the calculation of F_2. This plots have been produced with the HZTOOL analysis package [24]. Nice agreement with the data is observed for the case without the "consistency constraint". When the "consistency constraint" is applied, the prediction falls below the data. One has to note that in all cases the scale for α_s is k_t^2. Comparing this to the results in [16] the same trend is found: applying the "consistency constraint" and using k_t^2 as

the scale in α_s, the prediction of the cross section for forward jet production falls below the data, whereas there is essentially no effect seen in the prediction of the structure function F_2. It is interesting to note that the BFKL result of [16] (dashed curve in Fig. 4 of [16]) seems to be identical to the dashed line in Fig. 3 obtained from SMMOD.

3 Backward evolution: CCFM and CASCADE

The forward evolution procedure as implemented in SMALLX is a direct way of solving the CCFM evolution equation including the correct treatment of the kinematics in each branching. However the forward evolution is rather time consuming, since in each branching a weight factor is associated, and only after the initial state cascade has been generated completely, it can be decided whether the kinematics allow to generate the hard scattering process. Quite often, a complete event has to be rejected.

A more efficient procedure to be used in a full hadron level Monte Carlo is a backward evolution scheme, which is used in standard Monte Carlo programs [19,25] using a DGLAP type parton cascade. The idea is to first generate the hard scattering process with the initial parton momenta distributed according to the parton distribution functions. This involves in general only a fixed number of degrees of freedom, and the hard scattering process can be generated quite efficiently. Then, the initial state cascade is generated by going backwards from the hard scattering process towards the beam particles. In a DGLAP type cascade the evolution (ordering) is done usually in the virtualities of the exchanged t-channel partons.

According to the CCFM equation the probability of finding a gluon in the proton depends on three variables, the momentum fraction x, the transverse momentum squared k_t^2 of the exchanged gluons and the maximum angle allowed for any emission $P_{max} = x_{n-1}\sqrt{s\Xi}$. This probability distribution as a function of x, k_t^2 and P_{max} is obtained from a solution of the CCFM equation, here taken from the Monte Carlo procedure used in SMALLX and SMMOD as described in the previous chapter. For practical reasons the gluon density is obtained in a $50 \times 50 \times 20$ grid in $\log x$, $\log k_t$ and $\log P_{max}$, and then a linear interpolation method is used to obtain the gluon density at values in between the grid points.

However there is a problem in the normalization of the gluon density: In SMALLX and SMMOD the normalization is done via the momentum sum rule for all gluons below a given k_t for all P_{max}. But this P_{max} depends on the kinematics of the process involved. In order to obtain a gluon distribution, which is universal, the momentum sum rule is applied for each P_{max} separately. Therefore differences between SMMOD and the cross section calculated in the following are not surprising.

To fully simulate the hadronic final state of a small x process including the CCFM parton evolution, a new hadron level Monte Carlo program, CASCADE, has been developed. It consists of three steps:

- First the hard scattering process is generated:

$$\sigma = \int dk_t^2 dx_g \mathcal{A}(x_g, k_t^2, P_{max}) \sigma(\gamma^* g^* \to q\bar{q}) \tag{15}$$

where the off-shell matrix elements (given in [26, p. 178 ff]) are used, with the gluon momentum (in Sudakov representation):

$$k = x_g p_p + \bar{x}_g p_e + k_t \sim x_g p_p + k_t \tag{16}$$

The gluon virtuality k^2 is then $k^2 \sim k_t^2$.

- The initial state cascade is generated according to CCFM in a backward evolution approach (described in the next section).
- The hadronization is performed using the Lund string fragmentation implemented in JETSET [27–29].

At the present state, final state gluon radiation from both the quarks and the gluon p_i are neglected.

However in the backward evolution there is one difficulty: The gluon virtuality enters in the hard scattering process and also influences the kinematics of the produced quarks and therefore the maximum angle allowed for any further emission in the initial state cascade. This virtuality is only known after the whole cascade has been generated, since it depends on the history of the gluon evolution. In the evolution equations itself it does not enter, since there only the longitudinal energy fractions z_i and the transverse momenta are involved. This problem can only be approximatively overcome by using $k^2 = k_t^2/(1-x_g)$ for the virtuality which is correct in the case of no further gluon emission in the initial state.

The Monte Carlo program CASCADE can be used to generate unweighted full hadron level events, including initial state parton evolution according to the CCFM equation and the off - shell matrix elements for the hard scattering process. It is applicable both for photo production of heavy quarks as well as for deep inelastic scattering. The typical time for generating one event is ~ 0.03 sec, which is similar to the time needed by standard Monte Carlo event generators such as LEPTO [30] or PYTHIA [29]. In standard Monte Carlo generators [30,29], uncertainties concerning the scale to be used in the the structure functions and in α_s, and also the upper virtuality used in the parton shower approach are typical. As in SMMOD and SMALLX, in CASCADE, there are essentially no such free parameters left since everything is fixed by the requirement to describe the inclusive structure function F_2.

3.1 Backward evolution formalism

The CCFM evolution equation can be written [4,14,17] in a integral form as:

$$\mathcal{A}(x, k_t, P_{max}) = \mathcal{A}^0(x, k_t, P_{max}) + \int \frac{dz}{z} \int \frac{d^2q}{\pi q^2} \Theta(P_{max} - zq) \Delta_s(P_{max}, zq) \tilde{P}(z, q, k_t) \mathcal{A}(\frac{x}{z}, k_t', q) \tag{17}$$

with $k_t' = |\vec{k}_t + (1-z)\vec{q}|$ and with P_{max} being the upper scale for the last angle of the emission: $P_{max} > z_n q_n$, $q_n > z_{n-1} q_{n-1}$, ..., $q_1 > z_0 q_0 = Q_0$. Here q is used as a shorthand notation for 2-dimensional vector of the rescaled transverse momentum $\vec{q} = \vec{q}_t = \vec{p}_t/(1-z)$. The splitting function $\tilde{P}(z, q, k_t)$ is defined in eq.(9) and the Sudakov form factor $\Delta_s(P_{max}, zq)$ is given in eq.(8). The first term in eq.(17) can be expressed as:

$$\mathcal{A}^0 = G_0(x, k_t^2) \Delta_s(P_{max}, k_0) \tag{18}$$

with $G_0(x,k_t^2)$ defined in eq.(6) and k_0 being the starting scale for the evolution. Thus $\mathcal{A}^0$ gives the probability of moving from x_0, k_{t0} and k_0 to x, k_t and P_{max} without further branching.

In a backward evolution, we start from gluon k_n (see Fig. 1) and go successively down in the ladder until we end up at gluon k_0. Therefore we need to reconstruct the branchings $k_i \to k_{i-1} + q_i$, where k_i refers to the four vector of the t-channel gluon closest to the hard interaction, k_{i-1} to the one closer to the proton and q_i to the gluon emitted between i and $i-1$. The momenta of such a branching with given x_i, k_{ti} and q_{i+1} are reconstructed as follows:[3]

a. The value $\tilde{q}_i = z_i q_i$ is calculated from $d^2\tilde{q}_i/\tilde{q}_i^2 \Delta_s(q_{i+1},\tilde{q}_i)$ with the Sudakov form factor defined in eq.(8). Note, that due to the angular ordering constraint only the product $z_i q_i$ can be obtained, whereas in the DGLAP case with transverse momentum ordering, q_i could be obtained already here.

b. Next the splitting variable $z_i = x_i/x_{i-1}$ needs to be generated. The correct splitting function given in eq.(9) cannot be used, since it involves the variable q_i (in the argument of α_s), which is not known at this stage. Thus, z_i is generated first according to a approximate splitting function P_{gg}^{appr}:

$$P_{gg}^{appr}(z_i,k_{ti}^2) = \frac{\bar{\alpha}_s(k_{ti})}{z_i} + \frac{\bar{\alpha}_s(q_{t\,min})}{1-z_i} \geq \tilde{P}_{gg} \tag{19}$$

which is always larger than the true splitting function. The limits on z_i are given by:

$$x_i \leq z_i \leq 1 - \frac{x_i Q_0}{q_{i+1}}.$$

Also the z range needs to be larger than the true one: $z_i < 1 - Q_0/q_i$, but q_i is not determined at this stage. Having z_i generated, the true q_i can be calculated with $q_i = \tilde{q}_i/z_i$. If now $z_i > 1 - Q_0/q_i$, the branching is rejected, and a new one is generated by going back to step *a*.

c. Now the transverse momentum of gluon $(i-1)$ can be calculated, by generating a random angle ϕ around q_i: $k_{ti-1}^2 = k_{ti}^2 + q_{ti}^2 + 2\sqrt{k_{ti}^2}\sqrt{q_{ti}^2}\cos\phi$.

d. A branching is accepted with the probability:

$$\frac{\tilde{P}(z_i,k_{ti}^2,q_i^2)}{P_{gg}^{appr}(z_i,k_{ti}^2)} \frac{x_{i-1}\mathcal{A}(x_{i-1},k_{ti-1}^2,q_i^2)}{x_i \mathcal{A}_{max}(x_i)}, \tag{20}$$

where $\mathcal{A}_{max}(x_i)$ is the maximum value, $\mathcal{A}$ can take for any value $x > x_i$ and any value of k_t^2, q_t^2.

This then completes the reconstruction of one branching. In the next branching generated the values of x_{i-1}, k_{ti-1} and q_{ti} play the role, the values x_i,k_{ti} and q_{ti+1} had before. The cascade ends, with the probability:

$$\frac{\mathcal{A}^0(x_{i-1},k_{ti-1}^2,q_i^2)}{\mathcal{A}(x_{i-1},k_{ti-1}^2,q_i^2)} \tag{21}$$

This means that a further branching would have come from the initial gluon distribution.

[3] I am very much grateful to G. Salam for suggesting this approach for a backward evolution.

Due to the complicated structure of the splitting function and $\mathcal{A}$, this procedure is quite inefficient. It can be considerably improved by a different procedure in step c in the selection of the ϕ angle and the transverse momentum k^2_{ti-1}: the angle ϕ is now selected according to the probability:

$$\frac{\mathcal{A}^0(x_{i-1}, k^2_{ti-1}, q^2_i)}{\mathcal{A}(x_{i-1}, k^2_{tmin}, q^2_i)} \tag{22}$$

where $k^2_{tmin} = k^2_{ti} + q^2_{ti} - 2\sqrt{k^2_{ti}}\sqrt{q^2_{ti}}$ is the minimum transverse momentum allowed in this branching. In step d the ratio of the parton densities (in eq.(20)) is then changed correspondingly to:

$$\frac{x_{i-1}\mathcal{A}(x_{i-1}, k^2_{tmin}, q^2_i)}{x_i \mathcal{A}_{max}(x_i)}.$$

This gives an improvement of a factor of ~ 2 in time.

As mentioned already above, the true virtuality of the t-channel gluons can only be reconstructed after the full cascade has been generated. Now by going from the last (closest to the proton) gluon, which has virtuality $k^2_0 = k_{t\,0}/(1 - x_0)$, forward in the cascade to the hard scattering process, the true virtualities of k^2_i are reconstructed. At the end, the gluon entering to the quark box will have a larger virtuality than without initial state cascade. Thus a check is performed, whether the production of the quarks is still kinematically allowed. If not, then the whole cascade is rejected, and the event without cascade is kept.

4 Results

In this section, results obtained from the hadron level Monte Carlo program CASCADE, described in the previous chapter, are compared to those from SMMOD. In all cases, no "consistency constraint" is applied. The unintegrated gluon distribution was obtained from SMMOD. At parton level, both programs are expected to be identical, but differences can occur because of normalization problems, the finite grid size used to define of the unintegrated gluon density, and the effect of the virtuality of the gluon entering the hard scattering process, which is not properly known in the backward evolution approach.

In Fig. 4 the cross section as a function of the rapidity of the quarks η_q, the quark transverse momentum p^q_t, the transverse momentum of the quark pair p^{pair}_t and the gluon transverse momentum k_t obtained from CASCADE are compared to the ones obtained from SMMOD (dashed line). A rather good agreement is obtained. Also shown is the multiplicity and the transverse energy flow as a function of rapidity for the gluons of the initial state cascade, and the prediction from SMMOD for comparison. This shows that both the cross section and the initial state cascade are well reproduced within the backward evolution approach. However, the differences seen are due to uncertainties in the determination of the gluon density function. Further improvements needed here to optimize the grid and the extraction of the gluon density.

In Fig. 5 the structure function F_2 obtained from CASCADE is compared to the one obtained from SMMOD (the same as the solid line in Fig. 2). At large Q^2 the results agree rather nicely, whereas at small Q^2 differences are seen, due to uncertainties in the normalization of the gluon distribution. In Fig. 6 the prediction of the cross section for forward jet production is shown. The parton level results from CASCADE are similar to the ones obtained from SMMOD, keeping in mind the differences already seen in F_2. Also shown are the hadron level results

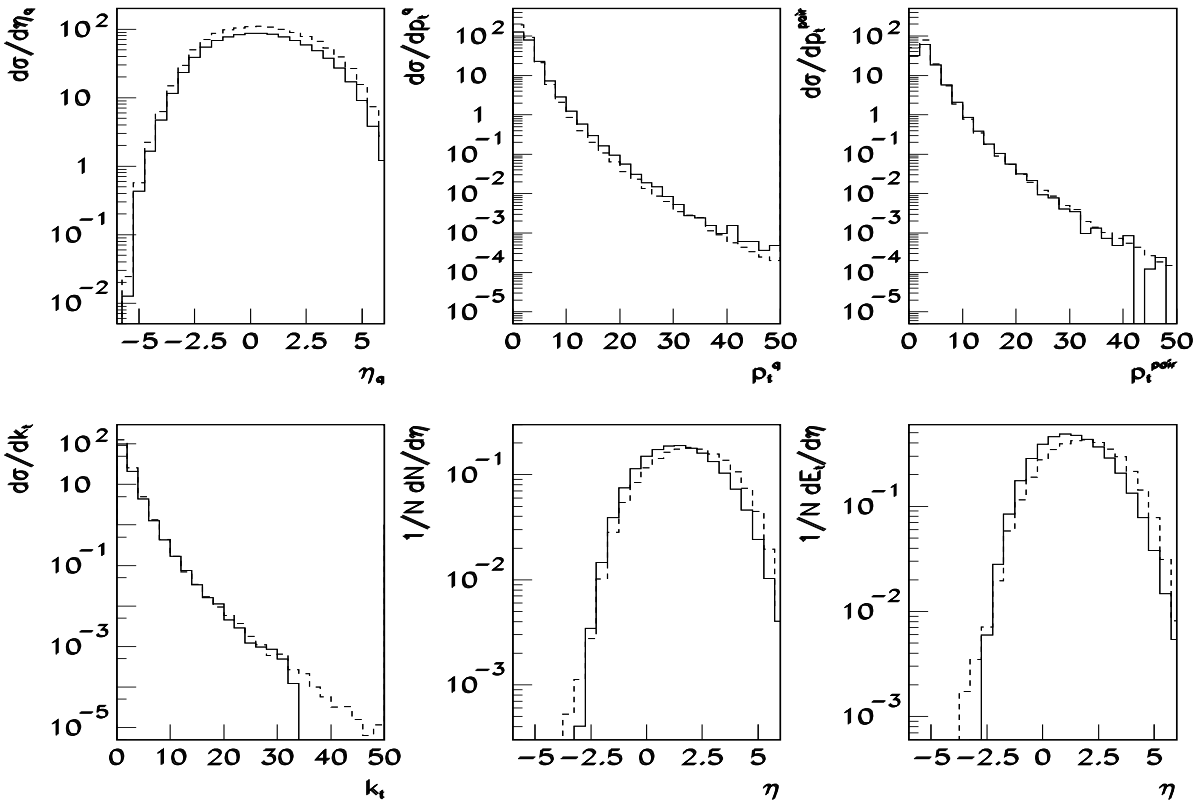

Figure 4: *Comparison of the cross section obtained from the backward evolution Monte Carlo* CASCADE *(solid line) with* SMMOD *(dashed line) both at parton level only. The upper 3 plots show the cross section is shown as a function of the quark rapidity η_q, the quark transverse momentum p_t and the transverse momentum of the quark pair p_t^{pair}. The lower 3 plots show the cross section as a function of the gluon transverse momentum k_t and the multiplicity and transverse energy flow of the gluons from the initial state cascade are shown as a function of the rapidity η*

from CASCADE, which differ from the parton level results by $\sim$ 20 %, which is known as the hadron level correction.

In Fig. 7 the transverse momentum distribution for single particles are shown in different bins of the rapidity. We observe a rather good description of the experimental measurements.

5 Conclusion

In this article I have shown, that the CCFM evolution equation with a proper treatment of the non-Sudakov form factor, gives a good description of the structure function F_2 and at the same time also describes the cross section for forward jet production. This results were obtained from SMMOD, a modified version of the forward evolution Monte Carlo program SMALLX [8,9], where the important change was the modified treatment of the non-Sudakov form factor. Whereas

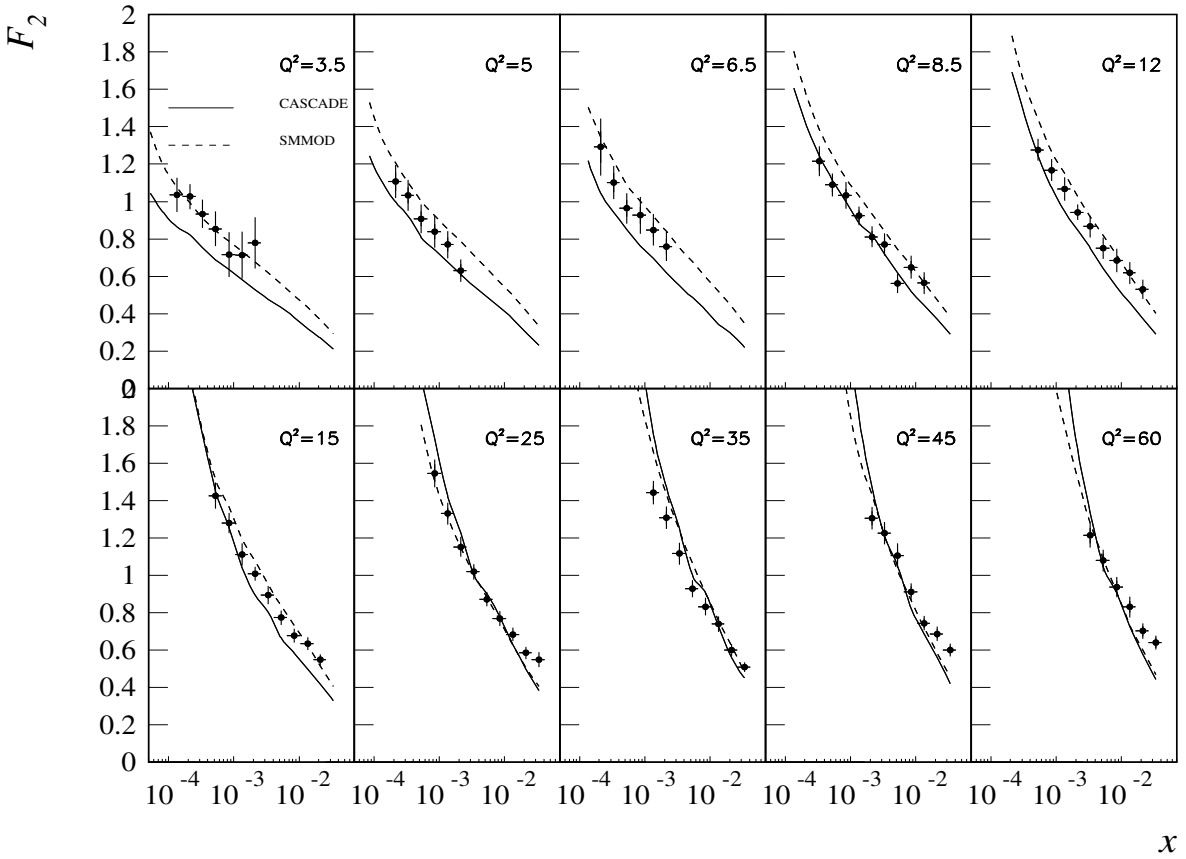

Figure 5: *Comparison of the structure function F_2 obtained from the backward evolution Monte Carlo* CASCADE *(solid line) with* SMMOD *(dashed line).*

for F_2 equally good descriptions are obtained with and without the "consistency constraint", the description of forward jet production improves if no "consistency constraint" is applied.

To fully simulate the hadronic final state of small x processes including parton emissions according to the CCFM evolution equation, a new hadron level Monte Carlo event generator, CASCADE, using a backward parton cascade approach, has been developed. The unintegrated gluon density as a function of x, k_t^2 and p^2 was obtained from SMMOD.

I have shown that the parton level results obtained from the forward evolution program SMMOD agree rather well with those from the backward evolution program CASCADE. The hadron level results obtained from CASCADE show rather nice agreement with measurements of the HERA experiments, that are sensitive to small x parton dynamics. With standard hadron level Monte Carlo programs using DGLAP type parton evolution and direct photon interactions only, a similar level of agreement could not be achieved.

6 Acknowledgments

I am very grateful to B. Webber for providing me with the SMALLX code, which was the basis of the studies presented here, and his patience to answer many questions about SMALLX. I

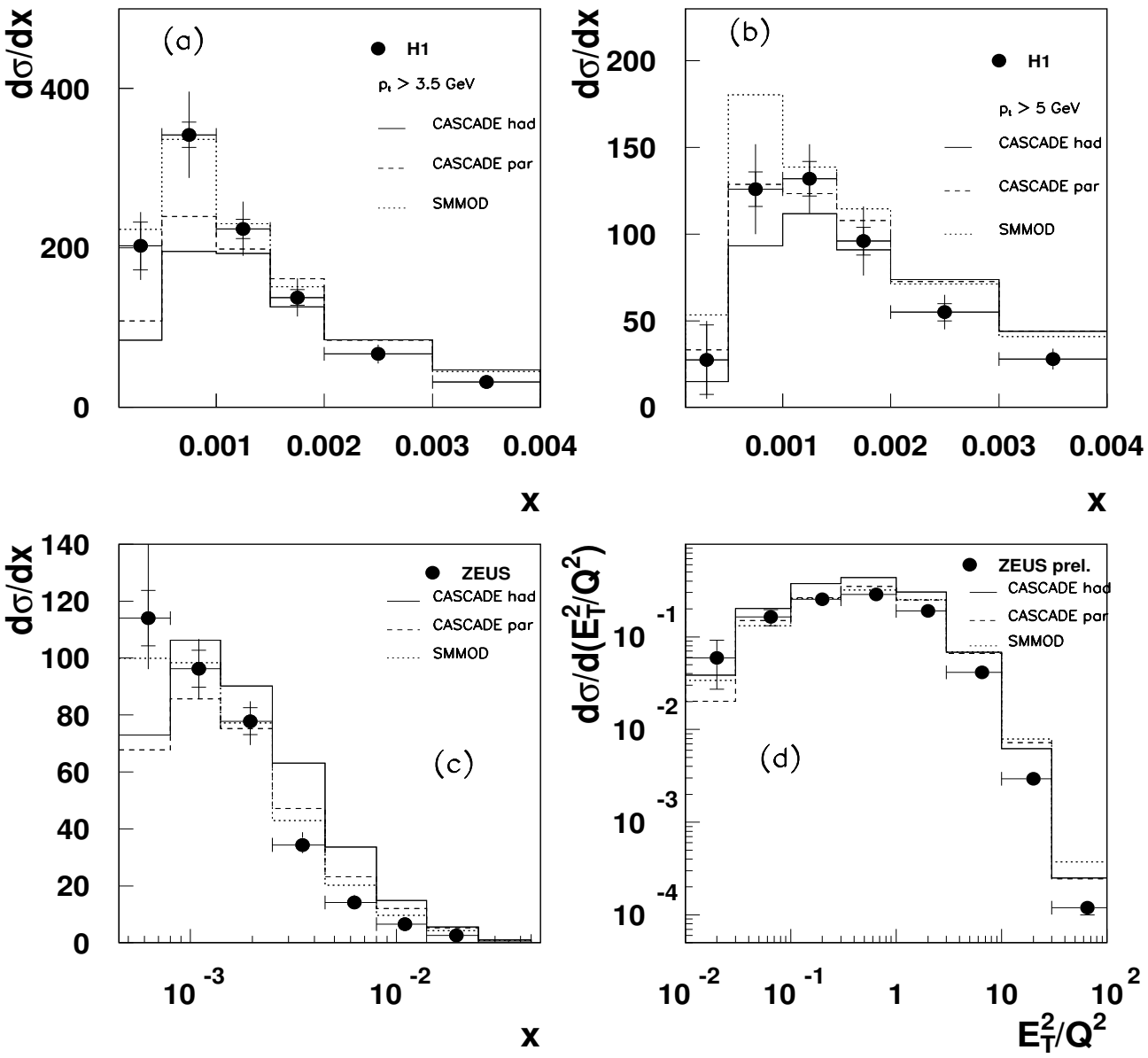

Figure 6: *Comparison of the cross section for forward jet production obtained from the backward evolution Monte Carlo* CASCADE *(dashed line) at parton level with* SMMOD *(dotted line) at parton level. Also shown is the prediction from* CASCADE *at hadron level (solid line). a.* $-$ *c. The cross section for forward jet production as a function of* x*, for different cuts in* p_t *compared to H1 data [21] (a.* $-$ *b.) and compared to ZEUS data [22] (c.). d. The cross section for forward jet production as a function of* E_T^2/Q^2 *compared to [23].*

am also very grateful to G. Salam, H. Kharraziha, L. Lönnblad for all their criticism and their clever and useful ideas on CCFM and the backward evolution. I have learned very much not only about CCFM from discussions with B. Andersson and G. Gustafson. I am also grateful to R. Peschanski and S. Munier for many discussions about CCFM, BFKL and the "consistency constraint" and the good times we always have in Paris. I also want to thank A.D. Martin and

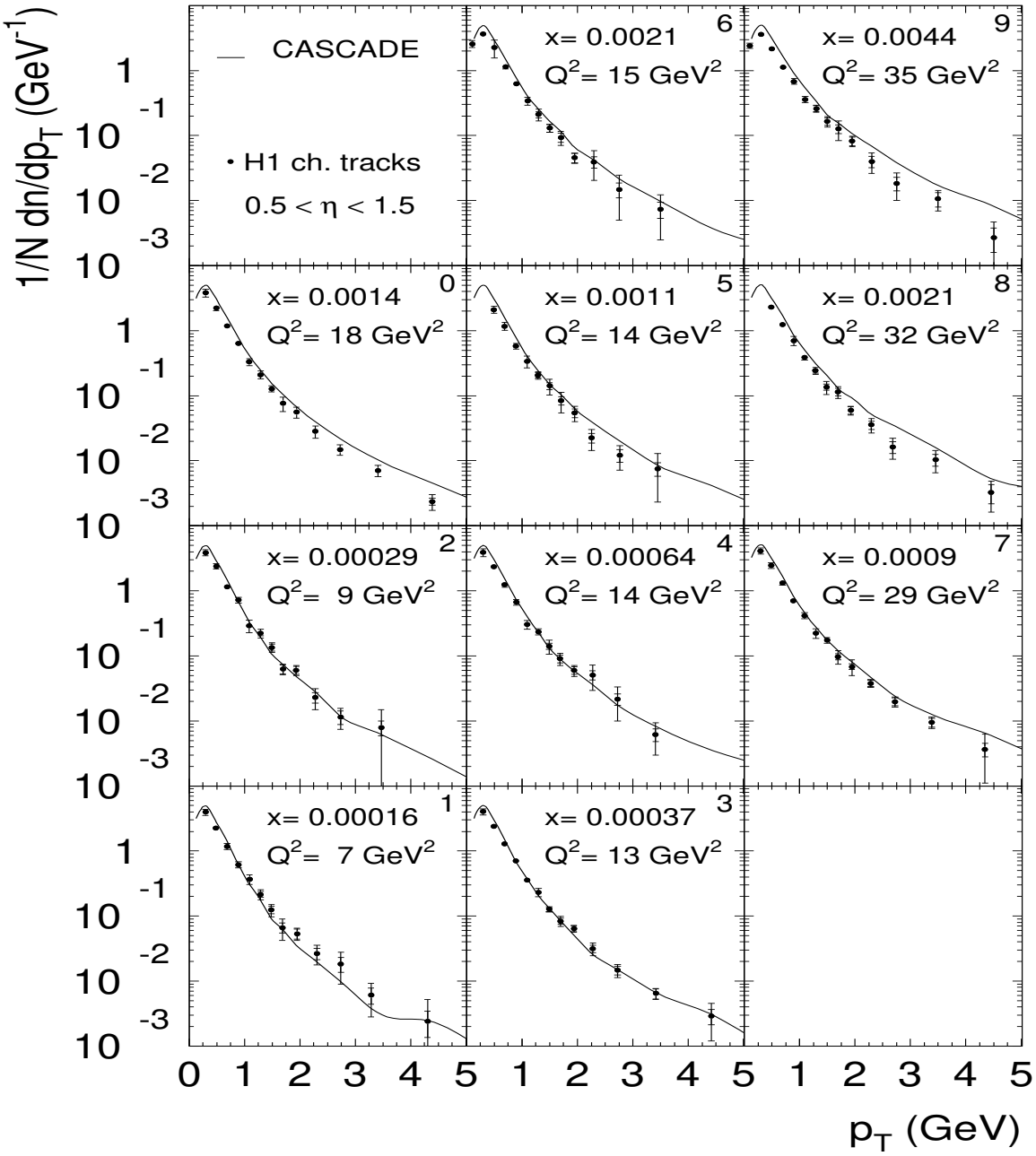

Figure 7: *The transverse momentum distribution of particles in different bins of rapidity. The prediction of the Monte Carlo* CASCADE *at hadron level is compared to the measurement of H1 [31]*

J. Kwiecinski for their explanation of the modified non - Sudakov form factor. I learned much from a continuous dialogue with G. Ingelman and T. Sjöstrand.

References

[1] M. Ciafaloni, *Nucl. Phys.* **B 296** (1988) 49.

[2] S. Catani, F. Fiorani, G. Marchesini, *Phys. Lett.* **B 234** (1990) 339.

[3] S. Catani, F. Fiorani, G. Marchesini, *Nucl. Phys.* **B 336** (1990) 18.

[4] G. Marchesini, *Nucl. Phys.* **B 445** (1995) 49.

[5] E. Kuraev, L. Lipatov, V. Fadin, *Sov. Phys. JETP* **44** (1976) 443.

[6] E. Kuraev, L. Lipatov, V. Fadin, *Sov. Phys. JETP* **45** (1977) 199.

[7] Y. Balitskii, L. Lipatov, *Sov. J. Nucl. Phys.* **28** (1978) 822.

[8] G. Marchesini, B. Webber, *Nucl. Phys.* **B 349** (1991) 617.

[9] G. Marchesini, B. Webber, *Nucl. Phys.* **B 386** (1992) 215.

[10] B. Andersson, G. Gustafson, J. Samuelsson, *Nucl. Phys.* **B 467** (1996) 443.

[11] B. Andersson, G. Gustafson, H. Kharraziha, J. Samuelsson, *Z. Phys.* **C 71** (1996) 613.

[12] G. Gustafson, H. Kharraziha, L. Lönnblad, The LCD Event Generator, in *Proc. of the Workshop on Future Physics at HERA*, edited by A. De Roeck, G. Ingelman, R. Klanner (1996), p. 620.

[13] H. Kharraziha, L. Lönnblad, *JHEP* **98003:006** (1998).

[14] G. Bottazi, G. Marchesini, G. Salam, M. Scorletti, *JHEP* **9812:11** (1998), hep-ph/9810546.

[15] L. Goerlich, J. Turnau, Some properties of the CCFM Monte Carlo SMALLX, in *Proc. of the Workshop on Monte Carlo Generators*, edited by A. Doyle, G. Grindhammer, G. Ingelman, H. Jung (1999).

[16] J. Kwiecinski, A. Martin, J. Outhwaite, *Eur. Phys. J.* **C** (1999), hep-ph/9903439.

[17] J. Kwiecinski, A. Martin, P. Sutton, *Phys. Rev.* **D 52** (1995) 1445.

[18] A. Bassetto, M. Ciafaloni, G. Marchesini, *Phys. Rep.* **100** (1983) 201.

[19] M. Bengtsson, T. Sjöstrand, M. van Zijl, *Z. Phys.* **C 32** (1986) 67.

[20] H1 Collaboration, S. Aid et al., *Nucl. Phys.* **B 470** (1996) 3.

[21] H1 Collaboration, C. Adloff et al., *Nucl. Phys.* **B 538** (1999) 3, DESY 98-143.

[22] ZEUS Collaboration; J. Breitweg et al., *Eur. Phys. J.* **C 6** (1999) 239, DESY 98-050.

[23] ZEUS Collaboration; J. Breitweg et al., Addendum to: Forward Jet Production in Deep Inelastic Scattering at HERA, Contributed paper to ICHEP98, Abstract 804, Vancover, 1998.

[24] N. Brook et al., HZTOOL - A Package for Monte Carlo Generator - Data comparison at HERA, in *Proc. of the Workshop on Future Physics at HERA*, edited by A. De Roeck, G. Ingelman, R. Klanner (1996), http://dice2.desy.de/ h01rtc/hztool.html.

[25] T. Sjöstrand, *Phys. Lett.* **B 157** (1985) 321.

[26] S. Catani, M. Ciafaloni, F. Hautmann, *Nucl. Phys.* **B 366** (1991) 135.

[27] T. Sjöstrand, *Comp. Phys. Comm.* **39** (1986) 347.

[28] T. Sjöstrand, M. Bengtsson, *Comp. Phys. Comm.* **43** (1987) 367.

[29] T. Sjöstrand, *Comp. Phys. Comm.* **82** (1994) 74.

[30] G. Ingelman, A. Edin, J. Rathsman, *Comp. Phys. Comm.* **101** (1997) 108.

[31] H1 Collaboration, C. Adloff et al., *Nucl. Phys.* **B 485** (1997) 3, DESY-96-215.